TSINGHUA SCIENCE AND TECHNOLOGY
ISSN 1007-0214 06/16 pp264-271
Volume 16, Number 3, June 2011

Covariances of Linear Stochastic Differential Equations for Analyzing Computer Networks*

FAN Hua (樊 华)[1,2,**], SHAN Xiuming (山秀明)[1], YUAN Jian (袁 坚)[1], REN Yong (任 勇)[1]

1. Department of Electronic Engineering, Tsinghua University, Beijing 100084, China;
2. Department of Cinematography, Beijing Film Academy, Beijing 100088, China

Abstract: Analyses of dynamic systems with random oscillations need to calculate the system covariance matrix, but this is not easy even in the linear case if the random term is not a Gaussian white noise. A universal method is developed here to handle both Gaussian and compound Poisson white noise. The quadratic variations are analyzed to transform the problem into a Lyapunov matrix differential equation. Explicit formulas are then derived by vectorization. These formulas are applied to a simple model of flows and queuing in a computer network. A stability analysis of the mean value illustrates the effects of oscillations in a real system. The relationships between the oscillations and the parameters are clearly presented to improve designs of real systems.

Key words: covariance matrix; stochastic differential equation (SDE); compound Poisson white noise; transmission control protocol (TCP) flow

Introduction

Stochastic differential equations (SDE) can be used to describe systems affected by random processes; however, the analyses of the SDE are very difficult, especially with nonzero noise at the equilibrium point of the deterministic solution. Such noise causes a non-negligible oscillation, so the estimate of this oscillation becomes very important. This paper presents formulas for the covariance matrix of a linear Itô SDE with additive compound Poisson noise or Gaussian white noise. The quadratic variation[1,2] is directly analyzed to derive the Lyapunov matrix differential equation which the covariance matrix obeys. The analysis then gives explicit formulas for the covariance matrix.

The results are used to analyze a computer network. The additive increase and multiplicative decrease (AIMD) algorithm used by the transmission control protocol (TCP) inevitably causes system oscillations. Although the SDE for the window size for a single TCP connection is known[3,4], researchers still do not know how to estimate the oscillations of the entire system. The main difficulty lies in writing the SDE for the aggregate flow and deriving the equations for the covariance matrix. The analysis in this paper uses an approximation up to the second order moment to derive the SDE with Poisson noise for the aggregate flow. Then the result is linearized to get a linear SDE. A stability analysis gives its covariance matrix which shows the effect of queue length variations on the system stability range.

Although the covariance matrix of the linear Stratonovich SDE with additive Gaussian white noise is known[5], that of the Itô SDE with additive Poisson noise is still unknown. Zygadlo[6] proved the Itô SDE covariance matrix cannot be derived explicitly from

Received: 2010-01-25; revised: 2011-04-22

* Supported by the National Natural Science Foundation of China (Nos. 60674048, 60772053, 60672142, and 60932005) and the National Key Basic Research and Development (973) Program of China (Nos. 2007CB307100 and 2007CB307105)

** To whom correspondence should be addressed.
E-mail: fanhua00@gmail.com; Tel: 86-10-82283460

the Stratonovich result. Grigoriu[7] proved that a real system with jumping noise conforms to the Itô SDE, instead of the Stratonovich SDE, to model the real physical process. The matrix equations presented here and the method used to handle the aggregate flow both provide new insights into the designs of real systems.

1 Covariance Matrix

Consider the following linear Itô SDE with additive compound Poisson noise:

$$\mathrm{d}\boldsymbol{X}(t)=\boldsymbol{A}\boldsymbol{X}(t)\mathrm{d}t+\boldsymbol{F}\mathrm{d}\boldsymbol{C}(t) \tag{1}$$

$$\boldsymbol{X}(0)=\boldsymbol{X}_0 \tag{2}$$

where $\boldsymbol{X}(t)$ is the state vector of an n-dimensional system, $\boldsymbol{A}$ is an $n\times n$ constant matrix, $\boldsymbol{F}$ is an $n\times m$ constant matrix, $\boldsymbol{C}(t)=(C_1(t),\cdots,C_m(t))^{\mathrm{T}}$ are m-dimensional independent compound Poisson processes defined in the following, the derivative conforms to Itô's definition, and $\boldsymbol{X}_0$ is the initial value which is an $n\times 1$ random vector independent of the compound Poisson processes. ($[\bullet]^{\mathrm{T}}$ denotes the transpose of $[\bullet]$.)

Each element of $\boldsymbol{C}(t)$ is a compound Poisson process defined as

$$C_i(t)=C(Y_i,\lambda_i,t)=\begin{cases}0, & N_i(t)=0;\\ \sum_{k=1}^{N_i(t)} Y_{ik}, & N_i(t)>0;\end{cases}\quad i=1,\cdots,m \tag{3}$$

where $C_i(t)$ depends on the independent identically distributed γ-valued random variables $\{Y_{ik}\}_{k=1}^{+\infty}$ which have the same distribution as the random variable Y_i and the homogeneous Poisson counting process $N_i(t)$ has intensity λ_i. $\{C_i(t)\}_{i=1}^{m}$ are mutually independent. $\{Y_i\}_{i=1}^{m}$ are also mutually independent.

Use the following symbols

$$\hat{\boldsymbol{C}}(t)\triangleq\mathbb{E}[\boldsymbol{C}(t)]=[\lambda_1\mathbb{E}[Y_1],\cdots,\lambda_m\mathbb{E}[Y_m]]^{\mathrm{T}}t\triangleq\boldsymbol{G}t,$$

where $\boldsymbol{G}=[\lambda_1\mathbb{E}[Y_1],\cdots,\lambda_m\mathbb{E}[Y_m]]^{\mathrm{T}}$ is an $m\times 1$ constant matrix. Here, $\hat{\boldsymbol{C}}(t)$ is the predictable quadratic variation (or predictable compensator) of $\boldsymbol{C}(t)$, so $\tilde{\boldsymbol{C}}(t)=\boldsymbol{C}(t)-\hat{\boldsymbol{C}}(t)$ is a martingale[1,2].

Theorem 1 The mean of system {(1), (2)} is

$$\mathbb{E}[\boldsymbol{X}(t)]=\mathrm{e}^{\boldsymbol{A}t}(\mathbb{E}[\boldsymbol{X}_0]+\boldsymbol{A}^{-1}\boldsymbol{F}\boldsymbol{G})-\boldsymbol{A}^{-1}\boldsymbol{F}\boldsymbol{G} \tag{4}$$

Iff $\boldsymbol{A}$ is stable (i.e., all eigenvalues of $\boldsymbol{A}$ have negative real parts), the mean converges and the limit is

$$\lim_{t\to+\infty}\mathbb{E}[\boldsymbol{X}(t)]=-\boldsymbol{A}^{-1}\boldsymbol{F}\boldsymbol{G} \tag{5}$$

Proof Taking the expectation of both sides of Eq. (1),

$$\mathrm{d}\mathbb{E}[\boldsymbol{X}(t)]=(\boldsymbol{A}\mathbb{E}[\boldsymbol{X}(t)]+\boldsymbol{F}\boldsymbol{G})\mathrm{d}t \tag{6}$$

The solution to this equation gives the theorem.

Theorem 2 The covariance of system {(1), (2)} is

$$\mathrm{Cov}[\boldsymbol{X}(t)]\triangleq\mathbb{E}[(\boldsymbol{X}(t)-\mathbb{E}[\boldsymbol{X}(t)])(\boldsymbol{X}(t)-\mathbb{E}[\boldsymbol{X}(t)])^{\mathrm{T}}]=$$

$$\mathrm{e}^{\boldsymbol{A}t}\mathrm{Cov}[\boldsymbol{X}_0]\mathrm{e}^{\boldsymbol{A}^{\mathrm{T}}t}+\int_0^t \mathrm{e}^{\boldsymbol{A}(t-s)}\boldsymbol{F}\boldsymbol{\varGamma}\boldsymbol{F}^{\mathrm{T}}\mathrm{e}^{\boldsymbol{A}^{\mathrm{T}}(t-s)}\mathrm{d}s \tag{7}$$

where $\boldsymbol{\varGamma}\triangleq\mathrm{diag}(\lambda_1\mathbb{E}[Y_1^2],\cdots,\lambda_m\mathbb{E}[Y_m^2])$ denotes a diagonal matrix whose diagonal entries are $\lambda_1\mathbb{E}[Y_1^2],\cdots,\lambda_m\mathbb{E}[Y_m^2]$.

Iff $\boldsymbol{A}$ is stable, the covariance matrix converges and the limit of the vectorization of the covariance matrix is

$$\lim_{t\to+\infty}\mathrm{vec}(\mathrm{Cov}[\boldsymbol{X}(t)])=$$

$$-(\boldsymbol{A}\otimes\boldsymbol{I}_n+\boldsymbol{I}_n\otimes\boldsymbol{A})^{-1}(\boldsymbol{F}\otimes\boldsymbol{F})\mathrm{vec}(\boldsymbol{\varGamma}) \tag{8}$$

where $\otimes$ is the Kronecker product, $\boldsymbol{I}_n$ is an identity matrix of size n, and $\mathrm{vec}(\bullet)$ is the column vectorization function.

Proof Using symbols $\hat{\boldsymbol{C}}$ and $\tilde{\boldsymbol{C}}$, Eq. (1) can be rewritten as

$$\mathrm{d}\boldsymbol{X}(t)=(\boldsymbol{A}\boldsymbol{X}(t)+\boldsymbol{F}\boldsymbol{G})\mathrm{d}t+\boldsymbol{F}\mathrm{d}\tilde{\boldsymbol{C}}(t).$$

Subtracting Eq. (6) from both sides gives:

$$\mathrm{d}(\boldsymbol{X}-\mathbb{E}[\boldsymbol{X}])=\boldsymbol{A}(\boldsymbol{X}-\mathbb{E}[\boldsymbol{X}])\mathrm{d}t+\boldsymbol{F}\mathrm{d}\tilde{\boldsymbol{C}} \tag{9}$$

From now on, the symbol t is omitted when the meaning is clear to make the expression more compact. The term $\boldsymbol{F}\mathrm{d}\tilde{\boldsymbol{C}}$ is the Itô calculus over a martingale, so the integral is also a martingale.

Integrating by parts using Itô calculus gives

$$\mathrm{d}((\boldsymbol{X}-\mathbb{E}[\boldsymbol{X}])(\boldsymbol{X}-\mathbb{E}[\boldsymbol{X}])^{\mathrm{T}})=\mathrm{d}(\boldsymbol{X}-\mathbb{E}[\boldsymbol{X}])\bullet$$

$$(\boldsymbol{X}-\mathbb{E}[\boldsymbol{X}])^{\mathrm{T}}+(\boldsymbol{X}-\mathbb{E}[\boldsymbol{X}])\bullet\mathrm{d}(\boldsymbol{X}-\mathbb{E}[\boldsymbol{X}])^{\mathrm{T}}+$$

$$\mathrm{d}[\boldsymbol{X}-\mathbb{E}[\boldsymbol{X}],(\boldsymbol{X}-\mathbb{E}[\boldsymbol{X}])^{\mathrm{T}}].$$

Taking the expectation of both sides with Eq. (9) and the martingale property of Itô calculus over the martingale $\tilde{\boldsymbol{C}}$ gives

$$\mathrm{d}\mathrm{Cov}[\boldsymbol{X}]=(\boldsymbol{A}\mathrm{Cov}[\boldsymbol{X}]+\mathrm{Cov}[\boldsymbol{X}]\boldsymbol{A}^{\mathrm{T}})\mathrm{d}t+$$

$$\boldsymbol{F}\bullet\mathrm{d}\mathbb{E}[[\tilde{\boldsymbol{C}},\tilde{\boldsymbol{C}}^{\mathrm{T}}]]\bullet\boldsymbol{F}^{\mathrm{T}} \tag{10}$$

The quadratic variation of $\tilde{\boldsymbol{C}}$ is[1,2]

$$[\tilde{C}_i,\tilde{C}_i](t)=[C_i,C_i](t)=\sum_{0<s\leqslant t}(\Delta C_i(s))^2=$$

$$\sum_{1<k\leqslant N_i(t)} Y_{ik}^2=C(Y_i^2,\lambda_i,t),$$

$$[\tilde{C}_i,\tilde{C}_j]=0,\quad \text{if } i\neq j.$$

Thus, the quadratic variation $[\tilde{C}_i,\tilde{C}_i](t)$ itself is also a compound Poisson process based on the same Poisson counting process $N_i(t)$ as $C_i(t)$, but with a random jump scale of Y_i^2 instead of Y_i. Thus,

$$\mathbb{E}[[\tilde{C}_i, \tilde{C}_i]] = \lambda_i \mathbb{E}[Y_i^2]t.$$

Using the definition of $\boldsymbol{\Gamma}$, Eq. (10) can be written as

$$\mathrm{dCov}[\boldsymbol{X}] = (\boldsymbol{A}\mathrm{Cov}[\boldsymbol{X}] + \mathrm{Cov}[\boldsymbol{X}]\boldsymbol{A}^{\mathrm{T}} + \boldsymbol{F\Gamma F}^{\mathrm{T}})\mathrm{d}t \quad (11)$$

This is a Lyapunov matrix differential equation. The solution gives Eq. (7).

When $t \to +\infty$, Eq. (11) becomes

$$\boldsymbol{0} = \boldsymbol{A}\mathrm{Cov}[\boldsymbol{X}(+\infty)] + \mathrm{Cov}[\boldsymbol{X}(+\infty)]\boldsymbol{A}^{\mathrm{T}} + \boldsymbol{F\Gamma F}^{\mathrm{T}} \quad (12)$$

Vectorization then gives Eq. (8).

Corollary 1 If the noise signals are all pure Poisson noise, let $Y_1 = \cdots = Y_m = 1$ a.s. (so that $\mathbb{E}[Y_i] = 1 = \mathbb{E}[Y_i^2]$), the Theorem 2 still works.

Proof Because iff $Y_i = 1$ a.s., the compound Poisson process C_i is a pure Poisson process.

Corollary 2 If the system in Eq. (1) is changed to

$$\mathrm{d}\boldsymbol{X}(t) = \boldsymbol{A}\boldsymbol{X}(t)\mathrm{d}t + \boldsymbol{F}\mathrm{d}\tilde{\boldsymbol{C}}(t) \quad (13)$$

where $\tilde{\boldsymbol{C}}(t) = \boldsymbol{C}(t) - \mathbb{E}[\boldsymbol{C}(t)] = \boldsymbol{C}(t) - \boldsymbol{G}t$ as defined before. The equations for the covariance matrix are still Eqs. (7) and (8).

Proof Note that $\boldsymbol{A}\boldsymbol{X}(t)\mathrm{d}t + \boldsymbol{F}\mathrm{d}\tilde{\boldsymbol{C}}(t) = (\boldsymbol{A}\boldsymbol{X}(t) - \boldsymbol{FG})\mathrm{d}t + \boldsymbol{F}\mathrm{d}\boldsymbol{C}(t)$. Since $-\boldsymbol{FG}$ is a constant vector, it remains in the equation for $\mathrm{d}\mathbb{E}[\boldsymbol{X}]$ but cancels in the equation for $\mathrm{d}(\boldsymbol{X} - \mathbb{E}[\boldsymbol{X}])$. Therefore, $-\boldsymbol{FG}$ does not affect the equations for the covariance process, but it does change the mean value process.

Now consider the following linear Itô SDE with additive Gaussian noise:

$$\mathrm{d}\boldsymbol{X}(t) = \boldsymbol{A}\boldsymbol{X}(t)\mathrm{d}t + \boldsymbol{D}\mathrm{d}\boldsymbol{B}(t) \quad (14)$$

$$\boldsymbol{X}(0) = \boldsymbol{X}_0 \quad (15)$$

where $\boldsymbol{X}(t)$ is the state vector of an n-dimensional system, $\boldsymbol{A}$ is an $n \times n$ constant matrix, $\boldsymbol{D}$ is an $n \times m$ constant matrix, $\boldsymbol{B}(t)$ is an m-dimensional independent Brownian motion where the derivative satisfies Itô's definition, and $\boldsymbol{X}_0$ is the initial value which is an $n \times 1$ random vector independent of the Brownian motion.

Theorem 3 The mean value of system {(14), (15)} is

$$\mathbb{E}[\boldsymbol{X}(t)] = \mathrm{e}^{\boldsymbol{A}t}\mathbb{E}[\boldsymbol{X}_0] \quad (16)$$

The covariance of system {(14), (15)} is

$$\mathrm{Cov}[\boldsymbol{X}(t)] = \mathrm{e}^{\boldsymbol{A}t}\mathrm{Cov}[\boldsymbol{X}_0]\mathrm{e}^{\boldsymbol{A}^{\mathrm{T}}t} + \int_0^t \mathrm{e}^{\boldsymbol{A}(t-s)}\boldsymbol{D}\boldsymbol{D}^{\mathrm{T}}\mathrm{e}^{\boldsymbol{A}^{\mathrm{T}}(t-s)}\mathrm{d}s \quad (17)$$

Iff $\boldsymbol{A}$ is stable, the mean converges to 0 and the covariance matrix converges to

$$\lim_{t\to+\infty} \mathrm{vec}(\mathrm{Cov}[\boldsymbol{X}(t)]) = -(\boldsymbol{A} \otimes \boldsymbol{I}_n + \boldsymbol{I}_n \otimes \boldsymbol{A})^{-1}(\boldsymbol{D} \otimes \boldsymbol{D})\mathrm{vec}(\boldsymbol{I}_m) \quad (18)$$

Proof The proof is similar with those of Theorems 1 and 2. The only difference lies in the quadratic variation of the Brownian motion:

$$\mathrm{d}[(\boldsymbol{X}(t) - \mathbb{E}[\boldsymbol{X}(t)]), (\boldsymbol{X}(t) - \mathbb{E}[\boldsymbol{X}(t)])^{\mathrm{T}}] =$$

$$\mathrm{d}[\boldsymbol{DB}(t), \boldsymbol{B}^{\mathrm{T}}(t)\boldsymbol{D}^{\mathrm{T}}] = \boldsymbol{D}\mathrm{d}[\boldsymbol{B}(t), \boldsymbol{B}^{\mathrm{T}}(t)]\boldsymbol{D}^{\mathrm{T}} = \boldsymbol{DD}^{\mathrm{T}}\mathrm{d}t.$$

Replacing $\boldsymbol{F\Gamma F}^{\mathrm{T}}$ in Eq. (11) by $\boldsymbol{DD}^{\mathrm{T}}$ then gives Eqs. (17) and (18).

2 SDE Model for the Aggregate Flow Using TCP

One of the important applications of covariance estimates in engineering systems is the analysis of TCP flows in computer networks. With the AIMD algorithm, both the TCP flows and the router queue length oscillate inevitably. The efficiency of the active queue management (AQM) algorithm then depends on estimates of these parameters, especially the router queue length. Accurate estimates of not only the mean queue length but also its variance will provide more precise operating parameter ranges to more effectively avoid congestion in the routers. The typical single bottleneck network shown in Fig. 1 is used as a simple example to illustrate the method.

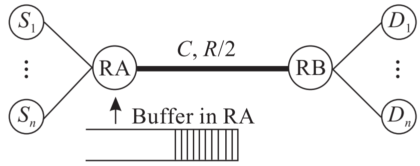

Fig. 1 A single bottleneck network

There are a total of n transmitters $S_1, \cdots, S_n$ sending endless ftp flows to the corresponding receivers $D_1, \cdots, D_n$ under TCP Reno. RA and RB are two routers connected by a communication link with bandwidth C and transmission delay $R/2$. We ignore the time delays between S_i and RA and between D_i and RB. Further assume that the processes on RB and all the receivers very fast and there is no congestion of the return ACK flows. It is then a typical system with a single bottleneck at router RA.

Misra et al.[3,4] gave the SDE with Poisson noise to describe the evolution of the window size for each single TCP connection:

$$\mathrm{d}W_t^{(i)} = \frac{1}{\mathrm{RTT}_t}\mathrm{d}t - \frac{W_{t-}^{(i)}}{2}\mathrm{d}N_t^{(i)}, \quad i = 1, \cdots, n \quad (19)$$

where $t-$ means the left limit of t (because there are jumps in the Poisson process), RTT_t is the round-trip time for instance t, $\{N_t^{(i)}\}_{i=1}^n$ are n independent identically-distributed Poisson processes denoting the arrival processes of congestion messages sent back to each transmitter, and $\{\mathcal{F}_t\}_{t\geqslant 0}$ is the filtration (or reference families) generated by these Poisson processes. These Poisson processes have the same intensities $\lambda_t^{(i)}=\lambda_t/n$ because the n transmitters are homogeneous. In addition, although λ_t is time-variant, it changes much more slowly than the system states due to the exponentially weighted moving average (EWMA) introduced in the following. Thus, when λ_t is calculated over a short period of time or near the fixed mean system value, λ_t can be treated as a time-invariant parameter. To further simplify the problem, Eq. (19) uses the delay-free assumption, ignores the slow start term, and only calculates the transmission delay and the queuing delay for the bottleneck node RA. Despite these simplifications, Misra et al.[3,4] have shown that their SDE model can quantitatively describe a real TCP connection.

This SDE for a single TCP connection is now extended to an SDE for the aggregate flow to reduce the number of SDEs for the entire system while modeling oscillations as precisely as possible. Summing up all the windows gives

$$W_t=\sum_{i=1}^n W_t^{(i)}.$$

Differentiating both sides and using Eq. (19) gives

$$\mathrm{d}W_t=\sum_{i=1}^n \mathrm{d}W_t^{(i)}=\frac{n}{R+\dfrac{Q_t}{C}}\mathrm{d}t-\frac{1}{2}\sum_{i=1}^n (W_{t-}^{(i)}\,\mathrm{d}N_t^{(i)}) \tag{20}$$

Since the Poisson processes have independent increments,

$$\mathbb{E}\left[\sum_{i=1}^n (W_{t-}^{(i)}\mathrm{d}N_t^{(i)})\,|\,\mathcal{F}_{t-}\right]=\frac{\lambda_t}{n}\sum_{i=1}^n W_{t-}^{(i)}\mathrm{d}t=\frac{\lambda_t}{n}W_{t-}\mathrm{d}t \tag{21}$$

$$\mathrm{Var}\left[\sum_{i=1}^n (W_{t-}^{(i)}\mathrm{d}N_t^{(i)})\,|\,\mathcal{F}_{t-}\right]=\frac{\lambda_t}{n}\sum_{i=1}^n (W_{t-}^{(i)})^2\,\mathrm{d}t \tag{22}$$

By the definition of the fairness index[8]

$$\sum_{i=1}^n (W_{t-}^{(i)})^2=a\frac{(W_{t-})^2}{n} \tag{23}$$

where a^{-1} is the fairness index. Many researchers have calculated this index using simulations. For general TCP flows, the fairness index is between 0.5 and 1, while for TCP/RED, it is often larger than 0.75[9]. Therefore, a is between 1 and 1.3. Then Eq. (22) can be rewritten as

$$\mathrm{Var}\left[\sum_{i=1}^n (W_{t-}^{(i)}\mathrm{d}N_t^{(i)})\,|\,\mathcal{F}_{t-}\right]=\frac{aW_{t-}^2\lambda_t}{n^2}\mathrm{d}t=\mathrm{Var}\left[\frac{\sqrt{a}W_{t-}}{n}\mathrm{d}\tilde{N}_t\,|\,\mathcal{F}_{t-}\right] \tag{24}$$

where $\tilde{N}_t=N_t-\int_0^t\lambda_s\mathrm{d}s$ and $N_t=\sum_{i=1}^n N_t^{(i)}$. Thus, N_t is a Poisson process with intensity λ_t and with $\tilde{N}_t$ as its corresponding Poisson martingale.

Combining Eqs. (21) and (24) gives an approximation of the random part of the total increment to the 2nd order moment,

$$-\frac{1}{2}\sum_{i=1}^n (W_{t-}^{(i)}\mathrm{d}N_t^{(i)})\approx-\frac{\lambda_t}{2n}W_t\,\mathrm{d}t-\frac{\sqrt{a}W_{t-}}{2n}\mathrm{d}\tilde{N}_t \tag{25}$$

Thus, Eq. (20) can be rewritten as

$$\mathrm{d}W_t=\left(\frac{n}{R+\dfrac{Q_t}{C}}-\frac{\lambda_t}{2n}W_t\right)\mathrm{d}t-\frac{\sqrt{a}W_{t-}}{2n}\mathrm{d}\tilde{N}_t \tag{26}$$

This describes the number of packets arriving at RA at time t, which is the window size for the aggregate flow.

In practice, routers use some algorithm to adjust λ_t according to the queue length to avoid congestion, such as random early detection (RED)[10]. TCP/RED can be modeled as a feedback control system[11]. The equation for the standard RED algorithm with EWMA is

$$\lambda_t=\frac{W_t}{\mathrm{RTT}_t}f(A_t)=\frac{W_t}{R+\dfrac{Q_t}{C}}f(A_t) \tag{27}$$

$$f(A_t)=\begin{cases}0, & A_t<q_{\min};\\ \dfrac{A_t-q_{\min}}{q_{\max}-q_{\min}}p_{\max}, & q_{\min}\leqslant A_t\leqslant q_{\max};\\ 1, & q_{\max}<A_t\end{cases} \tag{28}$$

$$\frac{\mathrm{d}A_t}{\mathrm{d}t}=\frac{n\ln(1-h)}{R+\dfrac{Q_t}{C}}(A_t-Q_t) \tag{29}$$

where Q_t is the router queue length, A_t is the exponentially weighted moving average of Q_t, h is a weight which generally equals 0.002 and $q_{\min}$, $q_{\max}$, and $p_{\max}$ are preassigned parameters[3].

The RED queue length performance can be improved by using explicit congestion notification (ECN)[12], where the original packet is transmitted forward as usual with only a notification sent back to its transmitter. ECN is used here to simplify the equation so that it can be solved explicitly.

$$\frac{\mathrm{d}Q_t}{\mathrm{d}t}=\begin{cases}\max\left\{\dfrac{W_t}{R+\dfrac{Q_t}{C}}-C,0\right\}, & Q_t=0;\\ \dfrac{W_t}{R+\dfrac{Q_t}{C}}-C, & 0<Q_t<\text{buff};\\ \min\left\{\dfrac{W_t}{R+\dfrac{Q_t}{C}}-C,0\right\}, & Q_t\geqslant\text{buff}\end{cases}\tag{30}$$

The primary equations in Eqs. (26), (30), and (29) plus the associated equations in Eqs. (27) and (28) give an integrated description of the aggregate flow in the network in Fig. 1 for TCP/RED control.

3 Stability Analysis of the Mean Value

The stability analysis of the system mean seeks to find the range of the number of connections n for which the system has a stable fixed mean.

The expectations of both sides of Eq. (26) are

$$\frac{\mathrm{d}W_t}{\mathrm{d}t}=\frac{n}{R+\dfrac{Q_t}{C}}-\frac{\lambda_t}{2n}W_t\tag{31}$$

The fixed operating point $(\hat{W},\hat{Q},\hat{A})$ of the system {(31), (30), (29)} in the three-dimensional space $[0,+\infty)\times[0,\text{buff}]\times[0,\text{buff}]$ is

$$\hat{A}=\hat{Q}\tag{32}$$

$$\hat{W}=\hat{Q}+CR\tag{33}$$

Only $0<\hat{A}=\hat{Q}\leqslant q_{\max}$ will give a reasonable fixed operating point. For this condition, $\hat{Q}$ obeys the equation

$$(\hat{Q}+CR)^2(\hat{Q}-q_{\min})=\frac{2n^2(q_{\max}-q_{\min})}{p_{\max}}\tag{34}$$

$\hat{Q}$ can then be determined either by using Cardano's formula or numerically.

From condition $0<\hat{Q}\leqslant q_{\max}$ and Eq. (34) gives Proposition 1.

Proposition 1 To ensure a reasonable fixed operating point for the system mean, the number of connections n has the upper bound

$$n\leqslant\sqrt{\frac{p_{\max}}{2}}(q_{\max}+CR)\tag{35}$$

For the stability analysis, linearize the SDE {(26), (30), (29)} near $(\hat{W},\hat{Q},\hat{A})$. Note that the random term in Eq. (26) is not zero at $(\hat{W},\hat{Q},\hat{A})$, so the solution includes the linear term for the deterministic term of the SDE and the constant term for the random term of the SDE. Thus, $\boldsymbol{X}_t\triangleq(W_t-\hat{W},Q_t-\hat{Q},A_t-\hat{A})^{\mathrm{T}}$,

$$\boldsymbol{\Phi}\triangleq\partial_{(W_t,Q_t,A_t)}\left.\left(\frac{n-\frac{K}{2n}(A_t-q_{\min})W_t^2}{R+\frac{Q_t}{C}},\frac{W_t}{R+\frac{Q_t}{C}}-C,\frac{n\ln(1-h)}{R+\frac{Q_t}{C}}(A_t-Q_t)\right)^{\mathrm{T}}\right|_{(W_t,Q_t,A_t)=(\hat{W},\hat{Q},\hat{A})}=$$

$$\begin{pmatrix}-\dfrac{K(\hat{A}-q_{\min})\hat{W}}{n\left(R+\dfrac{\hat{Q}}{C}\right)} & -\dfrac{n-\frac{K}{2n}(\hat{A}-q_{\min})\hat{W}^2}{C\left(R+\dfrac{\hat{Q}}{C}\right)^2} & -\dfrac{\frac{K}{2n}\hat{W}^2}{R+\dfrac{\hat{Q}}{C}}\\ \dfrac{1}{R+\dfrac{\hat{Q}}{C}} & -\dfrac{\hat{W}}{C\left(R+\dfrac{\hat{Q}}{C}\right)^2} & 0\\ 0 & -n\ln(1-h)\dfrac{R+\dfrac{\hat{A}}{C}}{\left(R+\dfrac{\hat{Q}}{C}\right)^2} & \dfrac{n\ln(1-h)}{R+\dfrac{\hat{Q}}{C}}\end{pmatrix}=\begin{pmatrix}\phi_1 & 0 & \phi_2\\ \phi_3 & -\phi_3 & 0\\ 0 & -\phi_4 & \phi_4\end{pmatrix},$$

where $K\triangleq p_{\max}/(q_{\max}-q_{\min})$, $\phi_1\triangleq-CK(\hat{Q}-q_{\min})$, $\phi_2\triangleq-CK(\hat{Q}+CR)/(2n)$, $\phi_3\triangleq C/(\hat{Q}+CR)$, $\phi_4\triangleq nC\ln(1-h)/(\hat{Q}+CR)$. This solution has substituted Eqs. (27) and (28) into Eq. (26), and the zero in the first row of the second column is due to Eqs. (32), (33), and (34).

$$\boldsymbol{\Psi}\triangleq\left.\begin{pmatrix}-\dfrac{\sqrt{a}W_t}{2n}\\ 0\\ 0\end{pmatrix}\right|_{(\hat{W},\hat{Q},\hat{A})}=\begin{pmatrix}-\dfrac{\sqrt{a}(\hat{Q}+CR)}{2n}\\ 0\\ 0\end{pmatrix}.$$

$$\hat{\lambda} = \frac{\hat{W}}{R + \dfrac{\hat{Q}}{C}} K(\hat{A} - q_{\min}) = CK(\hat{Q} - q_{\min}).$$

Then, the linearized equation of the stochastic system {(26), (30), (29)} is

$$\mathrm{d}\boldsymbol{X}_t = \boldsymbol{\Phi}\boldsymbol{X}_t \mathrm{d}t + \boldsymbol{\Psi}\mathrm{d}\tilde{N}_t \tag{36}$$

Some approximations give[13] Proposition 2.

Proposition 2 To ensure all the eigenvalues of $\boldsymbol{\Phi}$ have negative real parts, n should satisfy the following condition:

$$n > \frac{K(q_{\min} + CR)^3}{2\left(q_{\min} + CR + \dfrac{2}{h}\right)} \tag{37}$$

If there are no random oscillations in the system, i.e., Eqs. {(31), (30), (29)} are the exact system equations, Eqs. (35) and (37) can be used as the upper and lower bounds for the admission control in practice.

4 Covariance of the TCP/RED System

Real TCP/RED systems always have oscillations which affect the stability of the fixed operating point. The covariance matrix gives the amplitude of the random oscillations to understand the operations of real systems.

For the system in Eq. (36), let $\boldsymbol{V} \triangleq \lim_{t\to+\infty} \mathrm{Cov}[\boldsymbol{X}_t]$. From Corollary 2, $\boldsymbol{V}$ obeys Eq. (8). To further clarify, Eq. (12) in the proof of Theorem 2 can be used directly to get $\boldsymbol{0} = \boldsymbol{\Phi V} + \boldsymbol{V\Phi}^{\mathrm{T}} + \boldsymbol{\Psi}\hat{\lambda}\boldsymbol{\Psi}^{\mathrm{T}}$. Substituting $\boldsymbol{\Psi}$ and $\hat{\lambda}$ into the equation and using Eq. (34) gives

$$\boldsymbol{0} = \boldsymbol{\Phi V} + \boldsymbol{V\Phi}^{\mathrm{T}} + \begin{pmatrix} \dfrac{aC}{2} & 0 & 0 \\ 0 & 0 & 0 \\ 0 & 0 & 0 \end{pmatrix} \tag{38}$$

Thus, the covariance matrix $\boldsymbol{V}$ is approximately proportional to the bandwidth C (neglecting the nonlinear effect in $\boldsymbol{\Phi}$). Thus, when the bandwidth increases, the system loses its stability as shown by Low et al.[14] who did not clearly explain the cause because their model only included the deterministic part.

The result in Eq. (38) is compared with a real system for a simulated network using ns-2. The typical environmental parameters are: packetsize=1 KByte=8 Kb, C=24 Mbps=3 Kpackets/s, R=0.1 s, $q_{\min}$=800 Kb=100 packets, $q_{\max}$=2.4 Mb=300 packets, $p_{\max}=0.1$, $h=0.002$, buff=4.8 Mb=600 packets, and $a=1.1$. From Eqs. (35) and (37), the upper bound on the number of connections n is 134 and the lower bound is 12.

Then, calculate the covariance matrices $\boldsymbol{V}_n$ in Eq. (38) for n is 15, 75, and 130. $\boldsymbol{V}_n$ and the modified-correlation matrix $\boldsymbol{\Upsilon}_n$ for each n, which is the same as the correlation matrix except that the elements of the diagonal are the relative standard deviations (all these diagonal elements would be 1 for the correlation matrix.), are:

$$\boldsymbol{V}_{15} = \begin{pmatrix} 3806.0 & 3441.6 & -62.1 \\ 3441.6 & 3441.6 & 40.1 \\ -62.1 & 40.1 & 40.1 \end{pmatrix},$$

$$\boldsymbol{\Upsilon}_{15} = \begin{pmatrix} 0.1521 & 0.9509 & -0.1589 \\ 0.9509 & 0.5562 & 0.1079 \\ -0.1589 & 0.1079 & 0.0600 \end{pmatrix};$$

$$\boldsymbol{V}_{75} = \begin{pmatrix} 415.4 & 289.1 & 11.11 \\ 289.1 & 289.1 & 47.40 \\ 11.11 & 47.40 & 47.40 \end{pmatrix},$$

$$\boldsymbol{\Upsilon}_{75} = \begin{pmatrix} 0.0414 & 0.8342 & 0.0792 \\ 0.8342 & 0.0882 & 0.4049 \\ 0.0792 & 0.4049 & 0.0357 \end{pmatrix};$$

$$\boldsymbol{V}_{130} = \begin{pmatrix} 339.9 & 208.4 & 20.39 \\ 208.4 & 208.4 & 59.24 \\ 20.39 & 59.24 & 59.24 \end{pmatrix},$$

$$\boldsymbol{\Upsilon}_{130} = \begin{pmatrix} 0.0311 & 0.7831 & 0.1437 \\ 0.7831 & 0.0494 & 0.5331 \\ 0.1437 & 0.5331 & 0.0263 \end{pmatrix}.$$

The relative standard deviation of a random variable Z is defined as: $\mathrm{RSD}[Z] = \sqrt{\mathrm{Var}[Z]} / \mathbb{E}[Z]$. Both the variances and the relative standard deviations of W and Q decrease dramatically as n increases. For n near the lower bound, the variance of Q can not be neglected. Both the variance and the RSD of the EWMA variable A are much smaller than that of Q, which means that the oscillations of A are much smaller than that of Q, which is the objective of EWMA.

The relationship between the router queue length and the number of connections predicted by the present model are compared with those of a simulated system based on the mean ($\hat{Q}$) and the variance (the second row the second column of $\boldsymbol{V}$) as the number of connections increases. In the simulations, n was increased from 5 to 150 in steps of 5. Each step was simulated for 100 s with the last 25 s of the trajectory used to calculate the mean and the variance (the simulation time step was 0.05 s). The results are shown in Fig. 2 where the abscissa is the number of connections, n, and the ordinate is the queue length, Q. The two horizontal dotted lines denote $q_{\min}$ and $q_{\max}$. The two vertical dotted lines denote the lower bound n_{low} from Eq. (37) and the upper bound n_{up} from Eq. (35). The upper pair of curves is the mean Q_∞ calculated by the simulation (dashdotted curve) and by Eq. (34) (solid curve). The lower pair of curves are the standard deviations (the square root of the variance) of Q_∞ calculated by the simulation (dotted curve) and Eq. (38) (dashed curve).

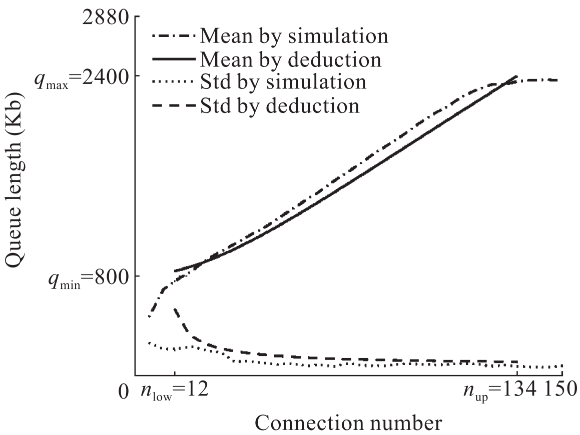

Fig. 2 Comparison of predicted and simulated queue length means and standard deviations

The results in this graph and in the modified-correlation matrices show that the variance can not be neglected relative to the mean, especially when n is near the lower bound. This means the random oscillation can destroy the system stability when n is slightly larger than the stable bound. This is the reason why previous studies have used some sufficient but not necessary assumptions for the parameter ranges for TCP/RED stability analyses when using the fluid flow model[15,16]. This study quantitatively shows the effects of the oscillations.

The results also show the current equations accurately model the real systems. The predicted standard deviation is always above the simulated curve, but is usually quite close. The predicted means are very close to the simulated values. The differences are due to many simplifications in the current derivations. For example, the real TCP uses the slow start algorithm to slow the increase of the transmission window size after receiving an ECN, which is neglected in the analyses. Also when the variance is large, the linearization precision decreases. Despite these simplifications, this model can still provide some useful insights into real systems.

Another important question is how the queue length standard deviation is affected by simultaneous system parameter changes. This effect is best shown in a multi-dimensional graph which is usually drawn from simulations which are very time consuming. The trends in Fig. 3 calculated using Eq. (38) illustrate the relationship between the queue length relative standard deviations, RSD, the number of connections, n, and the bandwidth, C. The result shows that RSD increases to a significant value as n decreases or C increases.

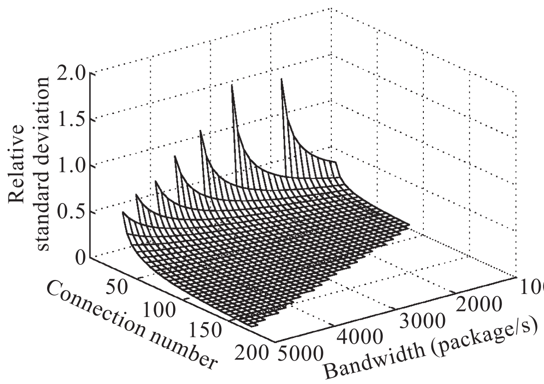

Fig. 3 Variation of the queue length relative standard deviation for various *n* and *C*

5 Conclusions

This paper presents equations for the covariance matrix of the linear SDE with additive Gaussian or compound Poisson noise. The equations can be used for many stochastic systems. A single bottleneck computer network using TCP/RED is used to illustrate the analysis of the variance. The system SDE is analyzed to determine the stability range of the mean queue length. The covariance matrix is then calculated for stable means. The results show how the stable system range estimated by the mean field method need to be adjusted, which is very important in the design of real engineering systems. The current results describe the statistical characteristics of the system operating state that are needed for better system designs.

References

[1] He Shengwu, Wang Jiagang, Yan Jiaan. Semimartingale and Stochastic Analysis. Beijing: Science Press, 1995: 242-250. (in Chinese)

[2] Ikeda N, Watanabe S. Stochastic Differential Equations and Diffusion Processes. 2nd ed. North-Holland, 1989: 53-72.

[3] Misra V, Gong Weibo, Towsley D. Stochastic differential equation modeling and analysis for TCP-window size behavior. ECE, Univ. of Massachusetts, MA, Tech. Rep. ECE-TR-CCS-99-10-01, 1999.

[4] Misra V, Gong Weibo, Towsley D. Fluid-based analysis of a network of AQM routers supporting TCP flows with an application to RED. In: Proc. ACM SIGCOMM'00. New York, NY, USA, 2000: 151-160.

[5] Shafiee M, Razzaghi M. On the solution of the covariance matrix differential equation for singular systems. *Intern. J. Computer Math.*, 1998, **68**: 337-343.

[6] Zygadlo R. Martingale integrals over Poissonian processes and the Ito-type equations with white shot noise. *Phys. Rev. E*, 2003, **68**: 046117.

[7] Grigoriu M. The Ito and Stratonovich integrals for stochastic differential equations with Poisson white noise. *Prob. Engng. Mech.*, 1998, **13**(3): 175-182.

[8] Chiu D M, Jain R. Analysis of the increase and decrease algorithms for congestion avoidance in computer networks. *Computer Networks and ISDN Systems*, 1989, **17**(1): 1-14.

[9] Reddy T B, Ahammed A. Performance comparison of active queue management techniques. *J. Computer Science*, 2008, **4**(12): 1020-1023.

[10] Floyd S, Jacobson V. Random early detection gateways for congestion avoidance. *IEEE/ACM Trans. Netw.*, 1993, **1**: 397-413.

[11] Firoiu V, Borden M. A study of active queue management for congestion control. In: Proc. IEEE INFOCOM. Tel Aviv, Israel, 2000: 1435-1444.

[12] Chung J, Claypool M. Analysis of active queue management. In: Proc. IEEE NCA. Cambridge, Massachusette, USA, 2003: 359-366.

[13] Fan Hua, Shan Xiuming. Using SDE to achieve the stable and statistical analyses for TCP/RED flows. In: Proc. WCICA. Jinan, China, 2010: 3565-3571.

[14] Low S H, Paganini F, Wang J, et al. Dynamics of TCP/RED and a scalable control. In: Proc. IEEE INFOCOM. 2002: 239-248.

[15] Hollot C, Misra V, Towsley D, et al. A control theoretic analysis of RED. In: Proc. IEEE INFOCOM. Anchorage, AK , USA, 2001: 1435-1444.

[16] Hollot C, Misra V, Towsley D, et al. Analysis and design of controllers for AQM routers supporting TCP flows. *IEEE Trans. Autom. Control*, 2002, **47**: 945-959.